Issue 39, 2021

From the journal:
Journal of Materials Chemistry C

Realizing nondestructive luminescence readout in photochromic ceramics *via* deep ultraviolet excitation for optical information storage †

Zetian Yang,[a] Jieqi Hu,[a] Lisa I. D. J. Martin,[a] David Van der Heggen *[a] and Dirk Poelman *[a]

* Corresponding authors

[a] LumiLab, Department of Solid State Sciences, Ghent University, Krijgslaan 281-S1, Ghent, Belgium

E-mail: david.vanderheggen@ugent.be

https://doi.org/10.1039/D1TC03946F

Realizing Nondestructive Luminescence Readout in Photochromic Ceramics via Deep Ultraviolet Excitation for Optical Information Storage

Zetian Yang, Jieqi Hu, Lisa I. D. J. Martin, David Van der Heggen* and Dirk Poelman*

LumiLab, Department of Solid State Sciences, Ghent University, Krijgslaan 281-S1, B-9000, Ghent, Belgium

Corresponding Authors

David Van der Heggen: E-mail address: david.vanderheggen@ugent.be; Full postal address: LumiLab, Department of Solid State Sciences, Ghent University, Krijgslaan 281-S1, B-9000, Ghent, Belgium.

Dirk Poelman: E-mail address: dirk.poelman@ugent.be; Full postal address: LumiLab, Department of Solid State Sciences, Ghent University, Krijgslaan 281-S1, B-9000, Ghent, Belgium.

Abstract

Photochromic materials exhibiting luminescence modulation behavior are regarded as promising for high-density optical information storage media. During the luminescence readout process however, many of these materials are subject to coloration or bleaching , which inevitably destroys the information encoded in the photochromic materials and hence inhibits their use in practical applications. Herein, we report a novel nondestructive luminescence readout in Ca_2SnO_4:Eu photochromic ceramics by selecting deep UV as the readout wavelength. The obtained Ca_2SnO_4:Eu ceramics show a reversible brown-gray color change together with a large reflectivity difference of 35 % upon alternating 280 nm and 585 nm illumination. Based on the photochromic behavior, a high luminescence modulation of 40.5 % with excellent cycling resistance was achieved upon 240 nm excitation without loss of data during the luminescence readout process. Wavelength- and power-dependent coloration and de-coloration processes were studied to obtain a deeper insight into the photochromic behavior. Furthermore, our proof-of-concept experiment demonstrates that Ca_2SnO_4:Eu ceramics are promising candidates for optical information storage and anti-counterfeiting applications. It is believed that these results will provide a good standard for designing other photochromic materials with nondestructive luminescence readout behavior.

Keywords: Photochromic ceramics, Ca_2SnO_4:Eu, luminescence modulation, optical information storage

1. Introduction

Photochromism is the photo-induced reversible transformation of a chemical species between two states whose absorption spectra are distinguishably different. Since the first report by J. Fritzsche in 1867, photochromic materials have been continually studied because of their promising applications ranging from optical information storage, over smart windows to anti-counterfeiting.[1-7] Up to now, the intensively studied photochromic materials can be divided into three categories: organic materials, inorganic materials and hybrid materials.[8-12] Although most reported photochromic materials are organic compounds by far, inorganic photochromic materials possess some inherent advantages over the organic-based materials in the aspects of thermal stability, chemical resistance and fatigue properties, and hence have attracted more attention in recent years.[13-21]

Currently, the research on inorganic photochromic materials mainly focuses on transition metal oxides (WO_3, MoO_3, TiO_2, Nb_2O_5 and V_2O_5),[22-27] ferroelectrics ($Na_{0.5}Bi_{4.5}Ti_4O_{15}$, $Na_{0.5}Bi_{2.5}Nb_2O_9$, $Bi_4Ti_3O_{12}$, $KSr_2Nb_5O_{15}$, $SrBi_2Nb_2O_9$ and $K_{0.5}Na_{0.5}NbO_3$),[10, 11, 18, 20, 21, 28-37] and other robust oxides ($BaMgSiO_4$, Sr_2SnO_4 and $(Ca,Sr,Ba)_5(PO_4)_3F$).[38-44] For these materials, light-induced changes in physical properties such as refractive index, electron conductivity, magnetic properties, refractive index or absorption spectrum can be regarded as the digital code of “0” and “1”, respectively.[30, 45] Correspondingly, the recorded information can be read out via measuring the change of those physical parameters such as luminescence intensity, refractive index and electrical conductivity.

Among these readout modes, detecting the change of luminescence intensity is regarded as the most promising method for practical applications because of its high resolution, large contrast and fast response speed. The luminescence readout mode in photochromic materials for optical memory mainly includes three processes, namely, “writing”, “reading” and “erasing”.[18] Normally, the writing and erasing processes are achieved using light corresponding to the coloring and bleaching bands of the photochromic process, respectively, while the reading process makes use of the typical excitation wavelengths of the luminescent ions. To verify this concept, a series of inorganic photochromic materials accompanied with luminescence modulation behavior have been developed in recent years such as $BaMgSiO_4$: M (M=Eu^{3+} or Bi^{3+}), $K_{0.5}Na_{0.5}NbO_3$: M (M=Sm^{3+}, Tb^{3+}, Dy^{3+}, Ho^{3+} or Eu^{3+}) and Sr_2SnO_4: M

(M=Sm^{3+}, Eu^{3+})[16, 29, 32, 45-52] For these photochromic materials with down-shifting luminescence properties, the recorded information can be read out through detecting the luminescence intensity, but new coloring also occurs due to the overlap between the luminescence excitation wavelength and the photochromic coloring band, and hence the written information is altered during the readout process, which is not desired in actual applications. For example, the information can be encoded in $BaMgSiO_4$: Eu^{2+} ceramics using light between 250 nm and 500 nm, while the luminescence readout process needs to be carried out upon 367 nm excitation, which damages the recorded information during the reading process.[46] To overcome this drawback, researchers proposed the strategy of a two-photon absorption process and developed various photochromic materials with up-conversion luminescence characteristic like $BaMgSiO_4$: Yb^{3+},Tb^{3+}, WO_3:Yb^{3+},Er^{3+}, $PbWO_4$:Yb^{3+},Er^{3+}, $Na_{0.5}Bi_{2.5}Nb_2O_9$: Yb^{3+}, Er^{3+}, $Na_{0.5}Bi_{2.5}Nb_2O_9$: Er^{3+}, $Ba_{0.7}Sr_{0.3}Nb_2O_6$: Er^{3+}, $K_{0.5}Na_{0.5}NbO_3$: Er^{3+}, $K_{0.5}Na_{0.5}NbO_3$: Nd^{3+} and Sr_2SnO_4: Er^{3+}.[11, 18, 27, 28, 35, 42, 43] For these materials, near-infrared light is selected as the excitation wavelength, which is separated from the coloring band, but it usually introduces new bleaching behavior, especially upon long illumination durations because of the overlap between the excitation wavelength and the bleaching band.[18] Consequently, although various inorganic photochromic materials exhibiting luminescence modulation behavior have been reported, achieving nondestructive luminescence readout, namely, without inducing any photochromic effects during the luminescence readout process, is still a challenging task.

As discussed above, the destructive luminescence readout of photochromic materials is mainly caused by the overlap between the luminescence excitation wavelength and the coloring band/bleaching band. Considering this, a suitable excitation wavelength, deviating from both the coloring and bleaching bands is required to avoid inducing photochromic effects during the readout process. For inorganic photochromic materials, the coloring wavelength is usually located between 250 nm to 500 nm, while the bleaching wavelength is usually longer than 450 nm in spite of slight differences in the coloring and bleaching bands for different materials.[16, 36, 42, 45, 46, 49] Based on this, selecting the deep ultraviolet (< 250 nm) for the reading process would be a good choice to achieve a nondestructive luminescence readout for photochromic materials if it can act as the excitation wavelength.

In this work, we report a Ca_2SnO_4:Eu ceramic as a new photochromic material, whose photoluminescence excitation spectrum possesses a broad peak from 235 nm to 330 nm due to the existence of a host charge transfer state.[53-55] Through systematic investigation of the wavelength-dependent coloration and de-coloration processes, it was found that Ca_2SnO_4:Eu ceramics can be colored and bleached by light in the range 250 - 360 nm and 585 - 810 nm, respectively, while 240 nm light has no effect on either the colored state or the uncolored state. Accordingly, 280 nm and 585 nm light were selected for the "writing" and "erasing" processes, respectively, while 240 nm light was used as the excitation wavelength to achieve a nondestructive luminescence readout. Upon alternate 280 nm and 585 nm illumination, a reversible brown-gray color change was observed in Ca_2SnO_4:Eu ceramics accompanied with an obvious change of reflectivity. More importantly, a nondestructive luminescence readout with a large luminescence contrast of 40.5 % and excellent cycling resistance was realized upon 240 nm excitation. These results confirm that selecting deep UV as the excitation wavelength can be an effective strategy to achieve nondestructive luminescence readout, which would give a guideline to design other high-performance photochromic materials with luminescence modulation behavior.

2. Experimental Section

2.1. Sample Preparation

$Ca_{1.995}Eu_{0.005}SnO_4$ (Ca_2SnO_4:Eu) ceramics were prepared by a conventional solid state method. Powders of $CaCO_3$ (Alfa Aesar, 99.95%), SnO_2 (Sigma Aldrich, 99.9%) and Eu_2O_3 (Alfa Aesar, 99.99%) were selected as the raw materials and weighed according to the chemical formula. 7.5 mol% of H_3BO_3 was added as the sintering aid. The raw materials were ball-milled with ethanol for 5 h at 300 rpm/min. After drying in an oven at 60 ^oC, the powders were first mixed with poly(vinyl alcohol) solution (5 wt %) and then pressed into pellets with a diameter of 13 mm and a thickness of ~1.2 mm. Finally, the green pellets were sintered at 1450 ^oC in air for 5 h to obtain dense ceramics.

2.2. Sample Characterization

Phase structures of the prepared ceramics were confirmed by powder X-ray diffraction (XRD) using a Siemens D5000 diffractometer (40 kV, 40 mA) with Cu Kα1 radiation (λ = 0.154 nm).

Scanning Electron Microscope (SEM) images and Energy-dispersive X-ray spectroscopy (EDS) were measured using a Hitachi S-3400N microscope, connected to a Thermo Scientific Noran 7 EDX analysis system, under a pressure of 25 Pa and an accelerating voltage of 20 kV. The reflectivity was measured using a PerkinElmer Lambda1050 UV-vis-NIR spectrophotometer equipped with a Spectralon-coated integrating sphere with PMT (photomultiplier) and InGaAs detectors. Steady state photoluminescence emission (PL) and photoluminescence excitation (PLE) spectra were measured using an Edinburgh FS920 (Edinburgh Instruments Ltd., Livingston, UK) fluorescence spectrometer equipped with a monochromated 450 W Xe-arc lamp as the excitation source. For the photochromic behavior, a NT340 series pulsed tunable laser (EKSPLA, Lithuania) and light emitting diodes (centered at 475 nm, 525 nm, 590 nm, 605 nm, 620 nm, 710 nm and 770 nm) were used as light sources.

3. Results and discussion

3.1 Structural properties

Figure 1a shows the XRD patterns of Ca_2SnO_4:Eu ceramics. All the diffraction peaks in the patterns well match the orthorhombic Ca_2SnO_4 structure with a space group of *Pbam* except for a small secondary phase of $CaSnO_3$, which usually formed during sintering of Ca_2SnO_4 ceramics.[56, 57] In addition, the absence of Eu-related impurity phase and the shift of the diffraction peaks to larger angles (see the insert of Figure 1a) indicate that the Eu^{3+} ions are well incorporated into the Ca_2SnO_4 lattice. Based on the ionic radius of Ca^{2+} (CN=7, R=1.06 Å), Sn^{4+} (CN=6, R=0.69 Å) and Eu^{3+} (CN=6, R=0.947 Å or CN=7, R= 1.01 Å),[58] it can be assumed that the Eu^{3+} ions tend to occupy the Ca^{2+} sites in the host lattice. Recent experiments and theoretical calculations have, however, shown that the doped Eu^{3+} ions can occupy either Ca^{2+} or Sn^{4+} sites, while the substitution of Eu^{3+} for the Ca^{2+} site dominates.[54, 59] Figure 1b displays the SEM image of Ca_2SnO_4:Eu ceramics. The surface morphology shows some large grains interspersed with a large number of small grains. The elements Ca, Sn and Eu are uniformly distributed in the samples, as confirmed by the EDS elemental mappings (see Figure1c-1e).

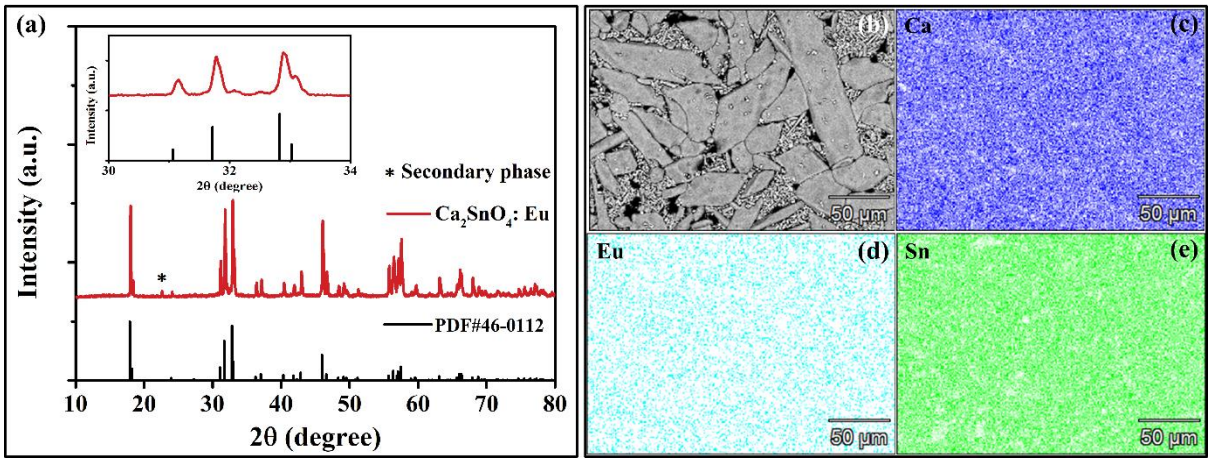

Figure 1. (a) XRD patterns of Ca_2SnO_4:Eu ceramics. (b) SEM images of Ca_2SnO_4:Eu ceramics. (c)-(e) Elemental mappings (Ca, Sn and Eu) of Ca_2SnO_4:Eu ceramics.

3.2 Photochromic properties

As the insert in Figure 2a shows, an obvious color change from brown to gray is observed in the Ca_2SnO_4: Eu ceramics after 280 nm illumination. Accompanied with the photochromic transition, an apparent decrease of reflectivity is obtained in Ca_2SnO_4:Eu ceramics (see Figure 2a), resulting in a large absorption band from 250 nm to ~1000 nm. Also, the sample's color and reflectivity can return to its original states upon 580 nm illumination, demonstrating a reversible photochromic behavior. For practical applications, the fatigue performance is an important parameter. Here, we selected 280 nm and 580 nm as the coloring and bleaching wavelength, respectively, and the corresponding reflectivity spectra of Ca_2SnO_4:Eu ceramics after different cycling times are shown in Figure S1. The reflectance at 664 nm is almost unchanged even after 15 cycles, as displayed in Figure 2b, demonstrating a good fatigue characteristic.

To determine the optimal wavelength to induce the photochromic process, the wavelength-dependency of the coloring process was studied and the results are shown in Figure 2c. Before each wavelength illumination, the sample was bleached to its original state, and a sufficiently long illumination time was applied for each wavelength to ensure that the sample reached the maximum colored state. The detailed reflectance spectra are provided in Figure S2a. Here, we adopted the reflectivity difference (ΔR) to evaluate the effectiveness of different wavelengths for the coloring process, which can be calculated by the following equation:

$$\Delta \mathrm{R} = R_0 - R_1 \quad (1)$$

where R_0 and R_1 represent the reflection intensity of the sample before and after illumination, respectively. As Figure S2b shows, the shape of the resulting absorption band is independent of the wavelength used to induce it, with the maximum position located at 664 nm. Figure 2c presents the reflectivity difference at 664 nm as a function of illumination wavelength. The sample can be colored by light with a wavelength between 250 nm and 360 nm, while no coloration behavior is observed upon 240 nm illumination. This phenomenon is caused by the absorption characteristics of the involved defects which mainly absorb light between 250 nm and 360 nm. The largest reflectivity difference was achieved upon 280 nm illumination with a value of 38.4 %, indicating that 280 nm is more effective than other wavelengths for the coloration process of Ca_2SnO_4: Eu ceramics. Correspondingly, a darker reflectance color is achieved in Ca_2SnO_4:Eu ceramics upon 280 nm illumination in comparison with that upon other wavelengths illumination, as shown in Figure 2e. For ferroelectric ceramics and robust oxides, the coloration process is associated with the trapping of vacancy-related traps.[46, 60, 61] In Ca_2SnO_4:Eu some defects are present which can act as traps for electrons or holes. The photochromic effect is due to an optically induced trapping of these charges under illumination with UV light.

Figure 2d displays the wavelength-dependent bleaching behavior of Ca_2SnO_4:Eu ceramics. Similar to the wavelength-dependent coloring processes, a sufficiently long illumination duration was applied for each wavelength to ensure that the sample reached a maximum possible bleached state. Prior to every measurement, the sample was switched to the colored state by illumination with 280 nm light. Here, we again selected the reflectivity change at 664 nm to see the wavelength-dependent bleaching processes. As shown in Figure 2d, the bleaching degree gradually enhances with illumination wavelength increasing from 425 nm to 525 nm. When the irradiation wavelength is greater than 585 nm, the reflectivity completely returns to the original state (see Figure S3) and the reflectivity difference at 664 nm is almost unchanged (see Figure 2d), indicating a complete bleaching is achieved. However, for wavelengths between 425 nm and 585 nm, two physical processes, namely, bleaching and coloring, coexist and a dynamic equilibrium will set in provided that the sample is illuminated for a sufficiently long time. This is evident from the overlap of the two curves shown in Fig. 2c and Fig. 2d. The trapping process gradually becomes weaker when the illumination wavelength increases,

resulting in a gradually enhanced bleaching degree. When the illumination wavelength is above 585 nm, only the de-trapping process remains and thereby the sample can be totally bleached.

While the results in Fig. 2d seem to suggest that all wavelengths above 585 nm can be used to completely bleach the samples if the sample is illuminated sufficiently long, it can be expected that some wavelengths will be more efficient or faster, than others. Therefore, the bleaching behavior of Ca_2SnO_4:Eu ceramics was investigated upon different illumination wavelengths (475 nm, 525 nm, 590 nm, 605 nm, 710 nm and 770nm) with the same power density (0.002 W cm^{-2}). Considering the low power density of the light source, it took a long time (> 30 min) to achieve a completely bleached state, so we only measured the initial bleaching process. As shown in Figure S4, a gradual increase of reflectivity is observed upon illumination at different wavelengths with increasing illumination time, while the reflectivity increase rate upon different wavelengths illumination is different. To compare the bleaching process upon different illumination wavelengths, Figure 2d presents the reflectivity difference at 664 nm as a function of bleaching wavelengths under the same illumination time (20 s and 60 s) and intensity. In general, under the same illumination time and the same power density, the bleaching upon shorter wavelength illumination is more effective than that upon longer wavelength illumination, while an exception is the bleaching behavior upon 525 nm and 590 nm illumination. As shown in Figure 2d, the bleaching effect under 590 nm illumination is better than that under 525 nm illumination in the initial bleaching stage (20 s), while the bleaching effect of 525 nm becomes stronger when the illumination time increases to 60 s. Under the same power-density illumination, the light of shorter wavelengths possesses less photons, while it exhibits a better bleaching effect. This indicates that under the same number of incident photons, more photons of shorter wavelength are absorbed by the sample to participate in the bleaching process. This phenomenon can be mainly ascribed to the larger absorbance of the sample in the shorter wavelength range in comparison with that of longer wavelengths. Figure S5 presents the absorbance of Ca_2SnO_4:Eu ceramics after 590 nm bleaching for different durations. In the initial stage, the absorbance at 590 nm is larger than that at 525 nm, resulting in a better bleaching effect upon 590 nm illumination in the initial stage (see Figure 2d blue line). When the illumination time increases, the absorbance at 525 nm becomes larger than that at 590 nm, leading to a better bleaching effect upon 525 nm

illumination (see Figure 2d red line). These results indicate that the bleaching effect of different wavelengths depends on the absorption characteristics of the material and the filled traps.

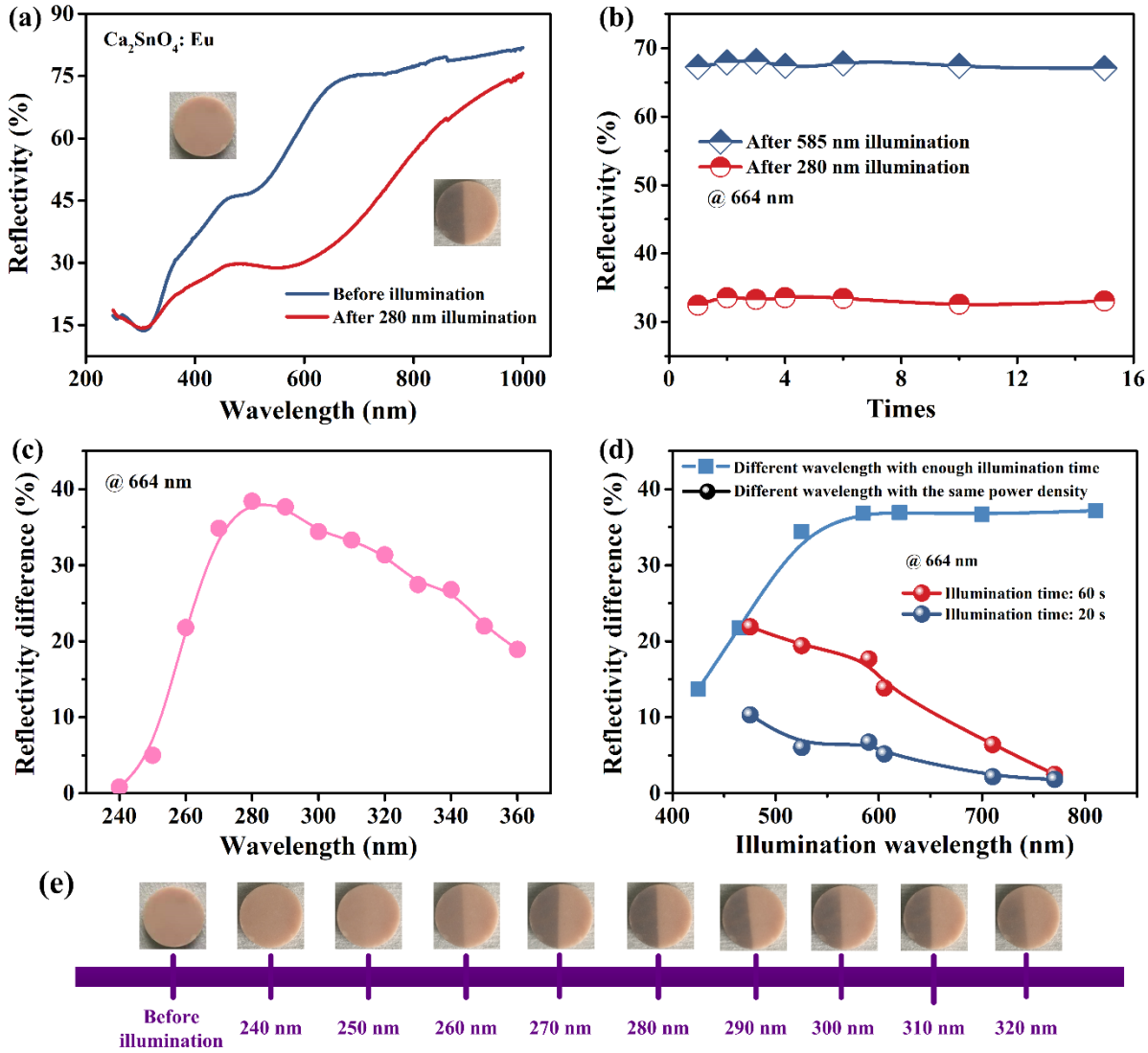

Figure 2. (a) Reflectivity of Ca_2SnO_4:Eu ceramics before and after 280 nm illumination. The insert displays the photograph of Ca_2SnO_4:Eu ceramics before and after 280 nm illumination. (b) Reflectivity of Ca_2SnO_4:Eu ceramics at 664 nm upon alternating 280 nm and 585 nm illumination as a function of cycling times. (c) Reflectivity difference at 664 nm as a function of the illumination wavelength. (d) Reflectivity difference of Ca_2SnO_4: Eu ceramics at 664 nm after reaching maximum bleaching as a function of bleaching wavelength, and after different wavelengths bleaching with the same power density and the same bleaching time. (e) Photographs of Ca_2SnO_4:Eu ceramics before and after illumination at different wavelengths.

To further illustrate the influence of illumination power density on the kinetics of

bleaching, the bleaching process of Ca_2SnO_4:Eu ceramics under 620 nm illumination with different power density was studied. A complete bleaching was achieved for all tested power-densities (see Figure S6a-S6c), since the chosen wavelength was larger than the 585 nm threshold. But, as expected, the time required to attain complete bleaching upon a low power-density illumination was relatively long. Figure 3a presents the reflectivity difference at 664 nm as a function of illumination time. The reflectivity difference at 664 nm increased approximately linearly in the initial illumination stage and then the increase rate gradually slowed down with increasing illumination time. Meanwhile, the increase rate of the reflectivity difference under a high power-density illumination was larger than that under a low power-density illumination. Figure 3b shows the change of absorbance difference at 664 nm in the initial illumination stage. Here, we selected the initial linear region to compare the bleaching process upon different power-density illumination, as indicated by the dashed lines in Figure 3b. As the illumination power density increased, the time required to reach the same absorbance difference decreased approximately proportionally. For example, the time required to reach a difference in absorbance of 0.15 upon 0.06 W cm^{-2}, 0.013 W cm^{-2} and 0.021 W cm^{-2} illumination was 8.8 s, 4.27 s and 3.06 s, respectively. The detailed data are provided in Table S1. These results indicate that the bleaching process of Ca_2SnO_4:Eu ceramics is power density-dependent and a faster bleaching can be expected upon higher power-density illumination.

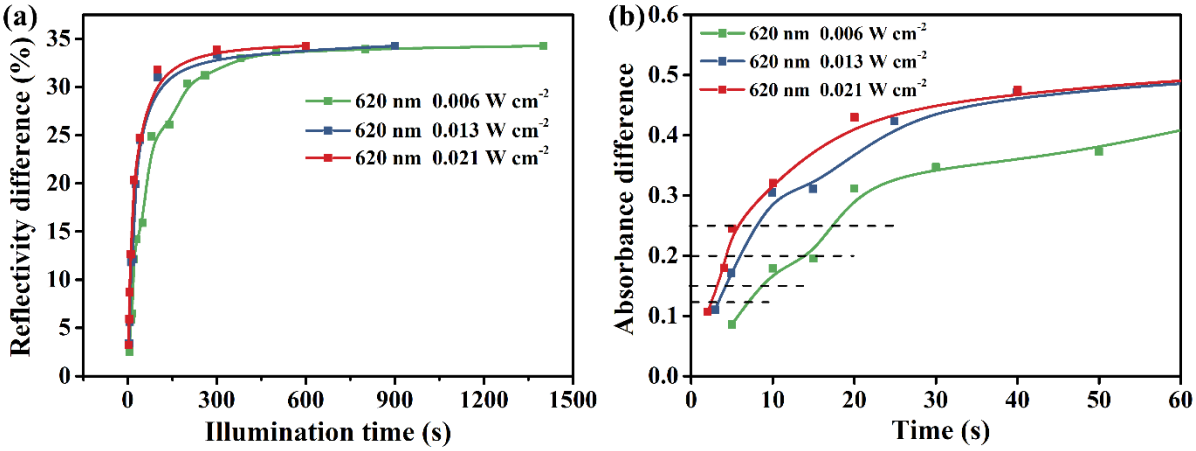

Figure 3. (a) Reflectivity difference of Ca_2SnO_4:Eu ceramics at 664 nm as a function of illumination time upon 620 nm bleaching with different power density. (b) Absorbance difference of Ca_2SnO_4:Eu ceramics at 664 nm as a function of illumination time.

3.3 Photochromism-induced luminescence modulation

Figure 4a displays the normalized PLE (λ_{em}=618 nm) and PL (λ_{ex}=240 nm) spectra of Ca_2SnO_4:Eu ceramics at room temperature. Monitored at 618 nm, the PLE spectrum consists of a broad band in the range from 235 nm to 330 nm and five sharp lines in the range from 350 nm to 470 nm, which correspond to the host charge transfer state (Eu^{3+} - O^{2-}) and the f-f transitions of Eu^{3+} ions ($^7F_0 \rightarrow {}^5D_4$ at 362 nm, $^7F_0 \rightarrow {}^5L_7$ at 382 nm, $^7F_0 \rightarrow {}^5L_6$ at 395 nm, $^7F_0 \rightarrow {}^5D_3$ at 415 nm, $^7F_0 \rightarrow {}^5D_2$ at 466 nm), respectively. Under 240 nm excitation, several emission peaks are observed, which originate from the $^5D_0 \rightarrow {}^7F_1$ (581, 586, 592 and 600 nm), $^5D_0 \rightarrow {}^7F_2$ (618 nm) and $^5D_0 \rightarrow {}^7F_3$ (656 nm) transitions of Eu^{3+} ions. During the photochromic processes, apart from the obvious color change, a large luminescence modulation can also be expected in some rare earth doped compounds due to the overlap between the emission band and the absorption band. However, although a reversible luminescence modulation has been achieved in many photochromic materials, a prominent problem for these materials is that the information will be erased during the luminescence readout process, which limits their applications in optical information storage. Such a phenomenon is also observed in Ca_2SnO_4:Eu ceramics by using 280 nm or 466 nm as the excitation wavelength during the luminescence readout process. For example, the coloring wavelength and the excitation wavelength of Ca_2SnO_4:Eu samples are at the same wavelength when using 280 nm as the excitation wavelength. This phenomenon indicates that the sample will be colored during the luminescence readout process, causing the information encoded in the sample to be damaged. Similarly, the colored sample will be bleached during the luminescence readout process by adopting 466 nm as the excitation wavelength due to the overlap between the excitation band and the bleaching band, resulting in an enhanced luminescence intensity and a bleaching of the information written in the sample, as shown in Figure 4b. In addition, although some photochromic materials with up-conversion luminescence characteristic have been designed to achieve a nondestructive luminescence readout by selecting the near-infrared light as the excitation wavelength, the colored sample will also be bleached after a long duration of illumination. To solve this problem, a suitable excitation wavelength, deviating from both the coloring band and the bleaching band, is required for the luminescence readout process. Figure 4c shows the effect of 240 nm illumination on both the colored and bleached states of

Ca_2SnO_4:Eu ceramics. The reflectivity spectra for both the colored and bleached state are unchanged after 240 nm illumination, indicating that 240 nm has no effect on the photochromic behavior of Ca_2SnO_4:Eu ceramics. As a result, 240 nm would be a suitable excitation wavelength for Ca_2SnO_4:Eu ceramics to achieve a nondestructive luminescence readout. To confirm this, we investigated the effect of 240 nm illumination on the luminescence behavior of Ca_2SnO_4:Eu ceramics. For both the colored and the bleached states, the PL spectra were first measured without 240 nm illumination and then measured again after 240 nm illumination. Also, the PL spectra measured before and after 240 nm illumination were measured under the same conditions by using 240 nm as the excitation wavelength. As shown in Figure S7, the luminescence intensity for both the colored and bleached state is unchanged after long illumination durations of 240 nm, indicating that a nondestructive luminescence readout can be realized in Ca_2SnO_4:Eu ceramics by selecting 240 nm as the excitation wavelength.

Figure 4d presents the PL spectra of Ca_2SnO_4:Eu ceramics before and after 280 nm illumination under 240 nm excitation. An apparent luminescence quenching behavior is observed in Ca_2SnO_4:Eu ceramics after photochromic behavior. The luminescence modulation degree (ΔI_l) can be defined by the following equation:

$$\Delta I_l = (I_0 - I_1)/I_0 \quad (2)$$

where I_0 and I_1 are the luminescence intensity before and after photochromism, respectively. Based on equation (2), the ΔI_l at 618 nm achieved in Ca_2SnO_4:Eu ceramics upon 240 nm excitation is 40.5 %. Also, the quenched luminescence intensity can return to its original intensity after 585 nm illumination (see Figure 4d), showing a reversible luminescence modulation behavior. The photochromism-induced luminescence modulation is ascribed to the energy transfer from the luminescent centers to the color centers. Before photochromism, Ca_2SnO_4:Eu ceramics exhibit several emission bands with certain luminescence intensities under a specific wavelength excitation. After photochromism, color centers are formed in Ca_2SnO_4:Eu ceramics, generating a broad absorption band from 250 nm to 1000 nm. Due to the overlap between the emission band and the absorption band, part of the energy from the luminescent centers will be transferred to the color centers to release the electrons captured by the defects via nonradiative relaxation processes, leading to a luminescence quenching behavior.[19, 49, 62, 63] In addition, the emission intensity detected at 618 nm for both the colored

and the bleached state is stable after four cycles, indicating that the luminescence modulation behavior achieved in Ca_2SnO_4:Eu ceramics possesses good fatigue properties. Also, compared with other photochromic materials ($Na_{0.5}Bi_{2.5}Nb_2O_9$, $Na_{0.5}Bi_{0.5}TiO_3$ and $K_{0.5}Na_{0.5}NbO_3$),[28, 33, 35, 63] the all optical-induced photochromic behavior makes Ca_2SnO_4:Eu ceramics exhibit obvious advantages in the aspects of easy accessibility and convenient control for practical applications.

As a proof a concept, the applications of Ca_2SnO_4:Eu ceramics in anti-counterfeiting and optical information storage were demonstrated. The sample was first covered with a mask exhibiting some “circular” holes and then illuminated by UV light. Due to the photochromic behavior, the “circular” patterns were encoded on the surface of the sample after 302 nm illumination, as shown in Figure 4e. This encoded information can also be read out in dark field upon 302 nm excitation. However, the encoded information can only be read out once in dark field upon 302 nm excitation, because the sample is colored during the luminescence readout process. As Figure 4e shows, the encoded information is damaged after using 302 nm as the excitation wavelength for the readout process. Differently, the encoded information can be read out several times by using 240 nm as the excitation wavelength since it has no effect on the photochromic behavior. As shown in Figure 4f, the encoded information remains on the sample after the luminescence readout process by using 240 nm as the excitation wavelength and it can be read out again. Using the difference in the readout behavior under different excitation wavelengths, Ca_2SnO_4:Eu ceramics can be used in anti-counterfeiting applications. In addition, the encoded information can be bleached upon 585 nm illumination and then the sample can be used to record information again. Together with the nondestructive luminescence readout behavior achieved upon 240 nm excitation, Ca_2SnO_4:Eu ceramic is a promising material for high-density information storage applications.

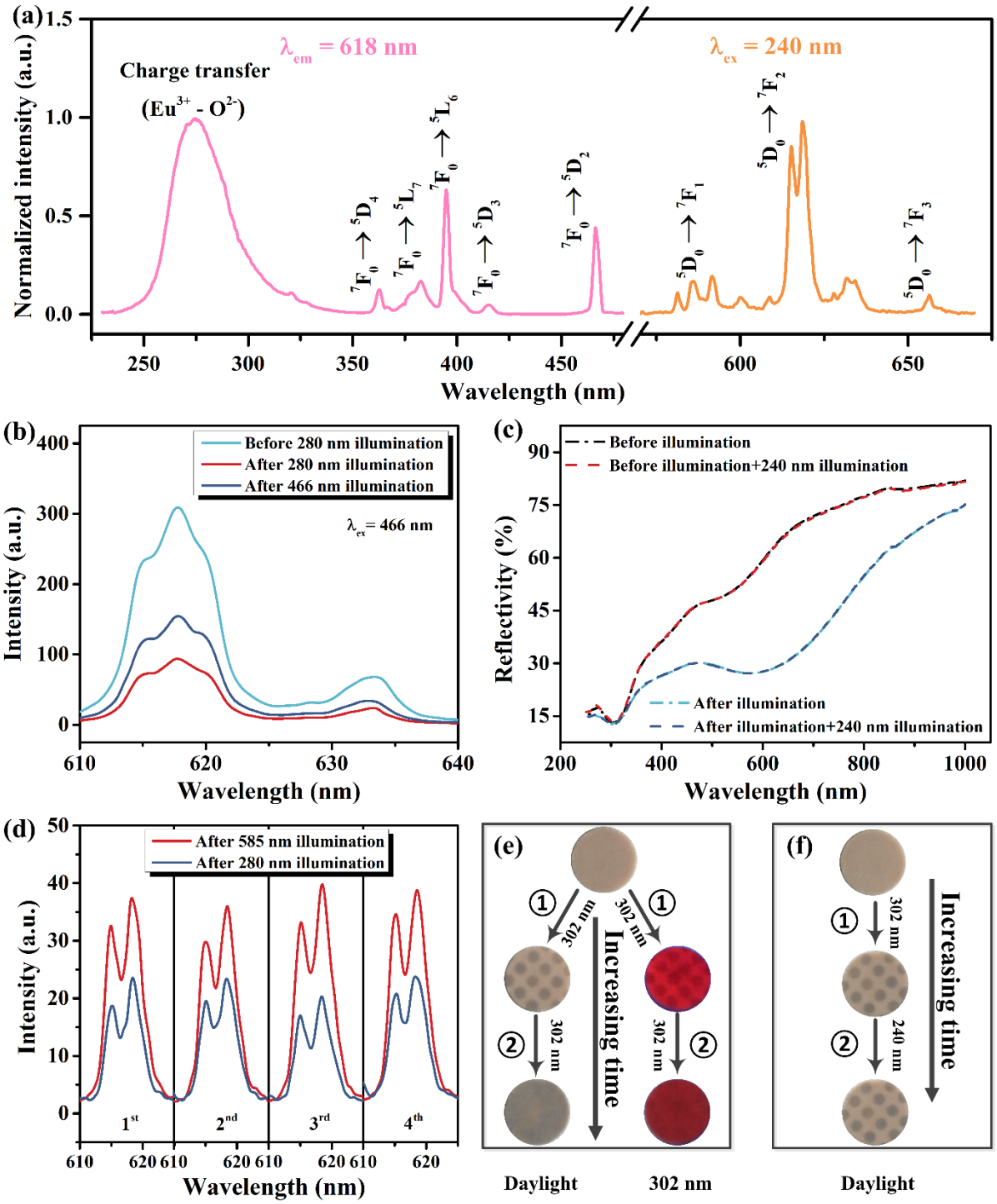

Figure 4. (a) Normalized PLE (λ_{em}=648 nm) and PL (λ_{ex}=240 nm) spectra of Ca_2SnO_4:Eu ceramics at room temperature. (b) PL (λ_{ex}=466 nm) spectra of Ca_2SnO_4:Eu ceramics at room temperature before 280 nm illumination, after 280 nm illumination and after 466 nm illumination in sequence with a illumination time of 2 min. (c) Reflectivity of Ca_2SnO_4:Eu ceramics before illumination, after 280 nm illumination, after 240 nm illumination on bleached samples and after 240 nm illumination on colored samples with a illumination time of 2 min.

(d) PL (λ_{ex} = 240 nm) spectra of Ca_2SnO_4:Eu ceramics after alternative 280 nm and 585 nm illumination as a function of the number of cycles, and the illumination time for 280 nm and 585 nm is 2 min and 5 min, respectively. (e) Optical information encoded in Ca_2SnO_4:Eu ceramics upon 302 nm illumination and the photographs after luminescence readout upon 302 nm excitation in daylight or 302 nm. (f) Optical information encoded in Ca_2SnO_4:Eu ceramics upon 302 nm illumination and the photographs after luminescence readout upon 240 nm excitation in daylight.

4. Conclusions

A new strategy of selecting deep UV as the excitation wavelength to achieve nondestructive luminescence readout in inorganic photochromic materials was proposed in this work. The obtained Ca_2SnO_4:Eu ceramics exhibit a reversible brown-gray color change upon alternate 280 nm and 585 nm illumination. Through systematically investigating the wavelength- and power-dependent coloration and de-coloration behavior of Ca_2SnO_4:Eu ceramics, it was found that the sample can be colored and bleached by the light in the range of 250-360 nm and 585-810 nm, respectively, while the deep UV of 240 nm has no effect on both the colored and the bleached state. Based on these behaviors, a nondestructive luminescence readout with a large luminescence contrast of 40.5 % and excellent fatigue properties is realized in Ca_2SnO_4:Eu ceramics by selecting 240 nm as the excitation wavelength. These interesting characteristics found in Ca_2SnO_4:Eu ceramics are superior to those of previously reported photochromic materials, endowing Ca_2SnO_4:Eu ceramics with great potential in optical information storage and anti-counterfeiting applications, and a prototype was presented to demonstrate the corresponding purposes. More importantly, this work provides an effective and feasible strategy to design other photochromic materials with a nondestructive luminescence readout behavior, which would promote the application of photochromic materials in various optical devices.

Conflicts of interest

There are no conflicts to declare.

Acknowledgements

Zetian personally acknowledges all the LumiLab members for their valuable discussions. The authors acknowledge the financial support from the FWO (project I002418N).

References

1. J. Zhang, Q. Zou and H. Tian, *Adv. Mater.*, 2013, **25**, 378-399.
2. T. He and J. Yao, *Prog. Mater. Sci.*, 2006, **51**, 810-879.
3. L. Wang and Q. Li, *Chem. Soc. Rev.*, 2018, **47**, 1044-1097.
4. S. Wang, W. Fan, Z. Liu, A. Yu and X. Jiang, *J. Mater. Chem. C*, 2018, **6**, 191-212.
5. Y. Ma, Y. Yu, P. She, J. Lu, S. Liu, W. Huang and Q. Zhao, *Sci. Adv.*, 2020, **6**, eaaz2386.
6. Z. Gao, Y. Han and F. Wang, *Nat. Commun.*, 2018, **9**, 3977.
7. A. Bianco, S. Perissinotto, M. Garbugli, G. Lanzani and C. Bertarelli, *Laser Photonics Rev.*, 2011, **5**, 711-736.
8. A. Julia-Lopez, D. Ruiz-Molina, J. Hernando and C. Roscini, *ACS Appl. Mater. Interfaces*, 2019, **11**, 11884-11892.
9. R. Samanta, D. Kitagawa, A. Mondal, M. Bhattacharya, M. Annadhasan, S. Mondal, R. Chandrasekar, S. Kobatake and C. M. Reddy, *ACS Appl. Mater. Interfaces*, 2020, **12**, 16856-16863.
10. Q. Zhang, Y. Zhang, H. Sun, W. Geng, X. Wang, X. Hao and S. An, *ACS Appl. Mater. Interfaces*, 2016, **8**, 34581-34589.
11. X. Bai, Z. Yang, Y. Zhan, Z. Hu, Y. Ren, M. Li, Z. Xu, A. Ullah, I. Khan, J. Qiu, Z. Song, B. Liu and Y. Wang, *ACS Appl. Mater. Interfaces*, 2020, **12**, 21936-21943.
12. C. T. Poon, W. H. Lam and V. W. Yam, *J. Am. Chem. Soc.*, 2011, **133**, 19622-19625.
13. S. Vuori, P. Colinet, I. Norrbo, R. Steininger, T. Saarinen, H. Palonen, P. Paturi, L. C. V. Rodrigues, J. Göttlicher, T. Le Bahers and M. Lastusaari, *Adv. Optical Mater.*, 2021, DOI: 10.1002/adom.202100762.
14. Z. Yang, J. Du, L. I. D. J. Martin, A. Feng, E. Cosaert, B. Zhao, W. Liu, R. Van Deun, H. Vrielinck and D. Poelman, *Adv. Optical Mater.*, 2021, DOI: 10.1002/adom.202100669.
15. C. Agamah, S. Vuori, P. Colinet, I. Norrbo, J. M. de Carvalho, L. K. Okada Nakamura,

J. Lindblom, L. van Goethem, A. Emmermann, T. Saarinen, T. Laihinen, E. Laakkonen, J. Lindén, J. Konu, H. Vrielinck, D. Van der Heggen, P. F. Smet, T. L. Bahers and M. Lastusaari, *Chem. Mater.*, 2020, **32**, 8895-8905.

16. J. Tang, P. Du, W. Li, G. Yuan, Z. Liu and L. Luo, *Chem. Eng. J.*, 2021, **410**, 128287.
17. X. Li, L. Guan, Y. Li, H. Sun, Q. Zhang and X. Hao, *J. Mater. Chem. C*, 2020, **8**, 15685-15696.
18. Q. Zhang, S. Yue, H. Sun, X. Wang, X. Hao and S. An, *J. Mater. Chem. C*, 2017, **5**, 3838-3847.
19. T. Wei, B. Jia, L. H. Shen, C. Z. Zhao, M. C. Wang, H. J. Zhang, Q. H. Hao, Q. J. Zhou and Y. H. Zhang, *Acta Mater.*, 2021, **205**, 116557.
20. S. Cao, F. Gao, J. Xu, J. Zhu, Q. Chen, Y. Guo, L. Li, J. Liu, T. Gao, E. Pawlikowska, M. Szafran and G. Cheng, *J. Eur. Ceram. Soc.*, 2019, **39**, 5260-5266.
21. J. F. Lin, P. Wang, H. J. Wang, Y. J. Shi, K. Zhu, F. Yan, G. H. Li, H. H. Ye, J. W. Zhai and X. Wu, *Adv. Optical Mater.*, 2021, DOI: 10.1002/adom.202100580.
22. P. Jittiarporn, L. Sikong, K. Kooptarnond and W. Taweepreda, *Ceram. Int.*, 2014, **40**, 13487-13495.
23. L. Pan, Y. Wang, X. Wang, H. Qu, J. Zhao, Y. Li and A. Gavrilyuk, *Phys. Chem. Chem. Phys.*, 2014, **16**, 20828-20833.
24. U. Joost, A. Šutka, M. Oja, K. Smits, N. Döbelin, A. Loot, M. Järvekülg, M. Hirsimäki, M. Valden and E. Nõmmiste, *Chem. Mater.*, 2018, **30**, 8968-8974.
25. J. Ruan, Z. Yang, A. Huang, H. Zhang, J. Qiu and Z. Song, *ACS Appl. Mater. Interfaces*, 2018, **10**, 14941-14947.
26. M. Bourdin, G. Salek, A. Fargues, S. Messaddeq, Y. Messaddeq, T. Cardinal and M. Gaudon, *J. Mater. Chem. C*, 2020, **8,** 9410-9421.
27. J. Ruan, Z. Yang, Y. Wen, M. Li, Y. Ren, J. Qiu, Z. Song and Y. Wang, *Chem. Eng. J.*, 2020, **383**, 123180.
28. Q. Zhang, X. Zheng, H. Sun, W. Li, X. Wang, X. Hao and S. An, *ACS Appl. Mater. Interfaces*, 2016, **8**, 4789-4794.
29. H. Sun, J. Liu, X. Wang, Q. Zhang, X. Hao and S. An, *J. Mater. Chem. C*, 2017, **5**, 9080-9087.

30. Q. Zhang, J. Liu, H. Sun, X. Wang, X. Hao and S. An, *J. Mater. Chem. C*, 2017, **5**, 807-816.
31. K. Li, L. Luo, Y. Zhang, W. Li and Y. Hou, *ACS Appl. Mater. Interfaces*, 2018, **10**, 41525-41534.
32. J. Lin, Y. Zhou, Q. Lu, X. Wu, C. Lin, T. Lin, K.-H. Xue, X. Miao, B. Sa and Z. Sun, *J. Mater. Chem. A*, 2019, **7**, 19374-19384.
33. H. Sun, X. Li, Y. Zhu, X. Wang, Q. Zhang and X. Hao, *J. Mater. Chem. C*, 2019, **7**, 5782-5791.
34. J. Bi, T. Wei, L. Shen, F. Yang, C. Zhao, M. Wang, Q. Yang and Y. Lin, *J. Am. Ceram. Soc.*, 2020, **104**, 1785-1796.
35. H. Wang, J. Lin, B. Deng, T. Lin, C. Lin, Y. Cheng, X. Wu, X. Zheng and X. Yu, *J. Mater. Chem. C*, 2020, **8**, 2343-2352.
36. T. Wei, B. Jia, L. Shen, C. Zhao, L. Wu, B. Zhang, X. Tao, S. Wu and Y. Liang, *J. Eur. Ceram. Soc.*, 2020, **40**, 4153-4163.
37. Z. Yang, J. Du, L. I. D. J. Martin, D. Van der Heggen and D. Poelman, *Laser Photonics Rev.*, 2021, **15**, 2000525.
38. J. M. Carvalho, I. Norrbo, R. A. Ando, H. F. Brito, M. C. A. Fantini and M. Lastusaari, *Chem. Commun.*, 2018, **54**, 7326-7329.
39. S. Kamimura, H. Yamada and C.-N. Xu, *Appl. Phys. Lett.*, 2013, **102**, 031110.
40. Y. Jin, Y. Hu, Y. Fu, L. Chen, G. Ju and Z. Mu, *J. Mater. Chem. C*, 2015, **3**, 9435-9443.
41. Y. Jin, Y. Lv, C. Wang, G. Ju, H. Wu and Y. Hu, *Sensor. Actuat. B-Chem.*, 2017, **245**, 256-262.
42. Y. Zhang, L. Luo, K. Li, W. Li and Y. Hou, *J. Mater. Chem. C*, 2018, **6**, 13148-13156.
43. Y. Ren, Z. Yang, M. Li, J. Ruan, J. Zhao, J. Qiu, Z. Song and D. Zhou, *Adv. Optical Mater.*, 2019, **7**, 1900213.
44. Y. Lv, Y. Jin, Z. Li, S. Zhang, H. Wu, G. Xiong, G. Ju, L. Chen, Z. Hu and Y. Hu, *J. Mater. Chem. C*, 2020, **8**, 6403-6412.
45. Y. Ren, Z. Yang, Y. Wang, M. Li, J. Qiu, Z. Song, J. Yu, A. Ullah and I. Khan, *Sci. China Mater.*, 2020, **63**, 582-592.
46. Y. Zhu, H. Q. Sun, Q. N. Jia, L. L. Guan, D. F. Peng, Q. W. Zhang and X. H. Hao, *Adv.*

Optical Mater., 2021, **9**, 2001626.

47. Q. Jia, Q. Zhang, H. Sun and X. Hao, *J. Eur. Ceram. Soc.*, 2021, **41**, 1211-1220.
48. C. Lin, H. J. Wang, P. Wang, X. Wu, T. F. Lin, B. S. Sa, Y. Cheng, X. H. Zheng, X. Yu and C. Q. Fang, *J. Am. Ceram. Soc.*, 2021, **104**, 903-916.
49. Z. Yang, J. Du, L. I. D. J. Martin and D. Poelman, *J. Eur. Ceram. Soc.*, 2021, **41**, 1925-1933.
50. Y. Zhou, P. Wang, J. Lin, Q. Lu, X. Wu, M. Gao, T. Lin, C. Lin and X. Zheng, *Dalton Trans.*, 2021, **50**, 4914-4922.
51. Y. Zhang, J. Liu, H. Sun, D. Peng, R. Li, C. Bulin, X. Wang, Q. Zhang and X. Hao, *J. Am. Ceram. Soc.*, 2018, **101**, 2305-2312.
52. Y. Zhang, L. Luo, K. Li, W. Li and Y. Hou, *J. Phys. D: Appl. Phys.*, 2018, **51**, 365102.
53. Y. Suzuki and M. Kakihana, *J. Am. Ceram. Soc.*, 2009, **92**, S168-S171.
54. T. Ishigaki, A. Torisaka, K. Nomizu, P. Madhusudan, K. Uematsu, K. Toda and M. Sato, *Dalton Trans*, 2013, **42**, 4781-4785.
55. L. Xia, T. Hu, H. Liu, J. Xie, S. U. Asif, F. Xiong and W. Hu, *J. Alloy. Compd.*, 2020, **845**, 156131.
56. G. Krieke, A. Antuzevics, K. Smits and D. Millers, *Opt. Mater.*, 2021, **113**. 110842.
57. K. Du, X.-Q. Song, J. Li, W.-Z. Lu, X.-C. Wang, X.-H. Wang and W. Lei, *J. Alloy. Compd.*, 2019, **802**, 488-492.
58. R. D. Shannon, *Acta Cryst.*, 1976, **32**, 751-767.
59. S. K. Gupta, K. Sudarshan, B. Modak, A. K. Yadav, P. Modak, S. N. Jha and D. Bhattacharyya, *J. Phys. Chem. C*, 2020, **124**, 16090-16101.
60. R. Zhang, Y. Jin, L. Yuan, H. Wu, G. Xiong, C. Wang, L. Chen and Y. Hu, *J. Lumin.*, 2021, **233**, 117922.
61. C. Wang, Y. Jin, Y. Lv, G. Ju, L. Chen, Z. Li, H. Duan and Y. Hu, *Sensor. Actuat. B-Chem.*, 2018, **262**, 289-297.
62. Q. Zhang, J. Tang, P. Du, W. Li, G. Yuan, Z. Liu and L. Luo, *J. Eur. Ceram. Soc.*, 2021, **41**, 1904-1916.
63. Q. Zhang, L. Luo, J. Gong, P. Du, W. Li and G. Yuan, *J. Eur. Ceram. Soc.*, 2020, **40**, 3946-3955.

Graphical abstract

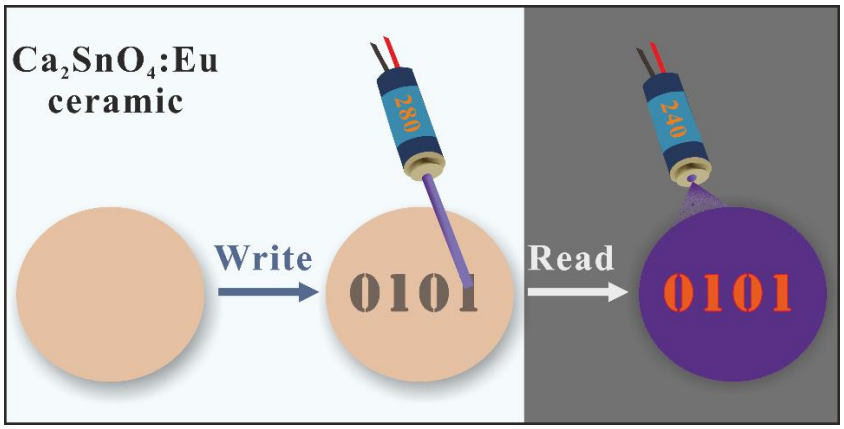

Through selecting deep ultraviolet as the excitation wavelength, a nondestructive luminescence readout together with a large luminescence modulation degree is achieved in Ca_2SnO_4:Eu photochromic ceramics, demonstrating great promise in optical information storage.